Research Square

Preprints are preliminary reports that have not undergone peer review.
They should not be considered conclusive, used to inform clinical practice,
or referenced by the media as validated information.

Systemic Tissue Colonization and Pathogenic Differentiation in Cucurbit-Associated Fusarium oxysporum from Taiwan

Yi-Jeng Chen
National Chiayi University - Lantan Campus: National Chiayi University
Chao-Jen Wang
Taichung District Agricultural Research and Extension Station
Ching-Chen Chung
National Chung Hsing University Department of Plant Pathology
Wen-Hsin Chung
wenchung@nchu.edu.tw

National Chung Hsing University https://orcid.org/0000-0002-8517-6368

Research Article

Keywords: Cotyledonary node, cross-pathogenicity, cucurbit crops, Formae speciales, host specificity, SIX6

Posted Date: September 24th, 2026

DOI: https://doi.org/10.21203/rs.3.rs-11007121/v1

License: This work is licensed under a Creative Commons Attribution 4.0 International License.
Read Full License

Abstract

Background

Fusarium oxysporum causes destructive wilt diseases in cucurbit crops and exhibits strong host specificity among different *formae speciales*. However, cross-pathogenicity has been reported among cucurbit-associated isolates, whereas its relationship with systemic tissue colonization across different biological contexts remains poorly understood. This study investigated the relationships among pathogenicity, systemic tissue colonization, and molecular characteristics of cucurbit-associated *F. oxysporum* isolates across different host species, environmental conditions, and propagation systems.

Results

Representative cucurbit-associated *F. oxysporum* isolates exhibited distinct pathogenicity and systemic tissue colonization patterns, with only limited cross-pathogenicity observed among host species. Across the evaluated host species, environmental conditions, and propagation systems, disease development was generally associated with systemic colonization beyond the cotyledonary node into the epicotyl, whereas weakly pathogenic or non-pathogenic interactions were predominantly associated with colonization confined to the hypocotyl. Temperature, host developmental stage, and grafting status influenced disease expression but did not substantially alter the overall patterns of systemic tissue colonization associated with pathogenic differentiation. Integrated analyses consistently grouped the isolates according to their pathogenicity and tissue colonization characteristics. Furthermore, phylogenetic analysis based on the *SIX6* gene was largely congruent with the biologically defined groupings and provided greater discriminatory power than the conserved IGS and *EF-1α* loci.

Conclusion

This study demonstrates that the ability to achieve systemic tissue colonization beyond the cotyledonary node is more closely associated with pathogenic differentiation among cucurbit-associated *F. oxysporum* isolates than with host origin alone. The integration of pathogenicity, tissue colonization, and SIX6 sequence analysis provides complementary biological and molecular evidence for characterizing pathogenic differentiation among cucurbit-associated *F. oxysporum* isolates and may facilitate resistance screening, rootstock evaluation, and disease management in cucurbit production systems.

Background

Fusarium wilt, caused by *Fusarium oxysporum*, is a major disease limiting the global production of Cucurbitaceae crops, which are economically vital and widely cultivated in tropical and subtropical regions (Tuttle McGrath, 2004). *F. oxysporum* is a genetically diverse species complex containing pathogenic and nonpathogenic strains that can persist in soil, water, or plant debris within agricultural

systems (van Dam et al. 2016; Zhang et al. 2020). As a plant pathogen, *F. oxysporum* generally exhibits a narrow host range and strong host specificity, with pathogenic diversity commonly classified into *formae speciales* (f. sp.) and races (Correll, 1991; O'Donnell et al. 1998). Currently, approximately 106 f. sp. have been recognized, and some are further subdivided into races with distinct virulence characteristics (Edel-Hermann and Lecomte, 2019).

Cucurbits represent one of the major host groups of *F. oxysporum*, with at least eight f. sp. identified, including *F. oxysporum* f. sp. *benincasae* (*Fob*), f. sp. *lagenariae* (*Fola*), f. sp. *niveum* (*Fon*), f. sp. *melonis* (*Fome*), f. sp. *cucumerinum* (*Foc*), f. sp. *radicis-cucumerinum* (*Forc*), f. sp. *luffae* (*Folu*), and f. sp. *momordicae* (*Fomo*), each associated with distinct cucurbit hosts (Lin et al. 2011). Strains within *Fon*, *Fome*, and *Foc* are further classified into distinct races (Martyn and Bruton 1989; Gwynne et al. 1997; Vakalounakis 1993). Although host specificity is a defining characteristic of *F. oxysporum*, cross-pathogenicity among f. sp. has been widely observed, particularly among phylogenetically related hosts or within the same plant family (Cafri et al. 2005; Alkher et al. 2009).

Cross-pathogenicity among cucurbit-infecting *F. oxysporum* isolates is relatively common. Several cucurbit-associated f. sp. can infect additional cucurbit hosts beyond their original hosts, including *Foc*, *Fome*, *Folu*, *Forc*, and *Fomo* (Armstrong and Armstrong 1978; Gerlagh and Blok 1988; Owen 1956; Palti and Joffe 1971; van Dam et al. 2016; Vakalounakis 1996). However, the occurrence and severity of cross-pathogenicity are influenced by multiple factors, including host genotype, infection pathway, environmental conditions, and plant developmental stage. For example, *Fome* exhibits variable pathogenicity among different melon and watermelon germplasms and infects cucumber following root-dip inoculation but not under soil infestation conditions (Cohen et al. 2015; Gerlagh and Blok 1988). Temperature is another important factor affecting disease development and host response; Folu and Fomo differ in their optimal temperatures for growth and symptom development, whereas *Forc* and *Foc* exhibit distinct temperature preferences for disease development on cucumber (Lin et al. 1996; Vakalounakis, 1996). In addition, host age has been reported to influence cross-pathogenicity, with cross-infection generally occurring more frequently in younger seedlings than in older plants (Gerlagh and Blok, 1988).

In Taiwan, Fusarium wilt caused by *F. oxysporum* is a major constraint in the production of vegetable cucurbits, including bitter gourd, cucumber, and sponge gourd. Owing to the strong host specificity among different *formae speciales*, grafting has become a common strategy for managing Fusarium wilt, with sponge gourd frequently used as a rootstock for bitter gourd (Wang et al. 2013). However, recent field observations of wilt symptoms in grafted plants have raised concerns regarding the host specificity and biological behavior of cucurbit-associated *F. oxysporum* isolates. Although cross-pathogenicity has been reported among several cucurbit-associated *formae speciales*, the relationships between pathogenicity, systemic tissue colonization, and host specialization under different host and environmental conditions remain poorly understood

Traditionally, differentiation of *F. oxysporum formae speciales* has relied largely on labor-intensive host inoculation assays. Although molecular markers such as the intergenic spacer (IGS) and *translation elongation factor 1-alpha* (*EF-1α*) are widely used for phylogenetic inference and species identification in *Fusarium*, these conserved loci often provide limited resolution for differentiating closely related *formae speciales*. In contrast, the virulence-associated *SIX* (secreted in xylem) genes have been reported to show stronger associations with host specificity and pathogenicity (Fraser-Smith et al. 2014; Jenkins et al. 2021; Lievens et al. 2009; O'Donnell et al. 1998; van Dam et al. 2016). Among them, *SIX1*, *SIX6*, and *SIX13* have demonstrated discriminatory potential among cucurbit-associated *formae speciales* (van Dam et al. 2018). Therefore, evaluating whether *SIX6*-based differentiation is consistent with biological characteristics may provide complementary evidence for characterizing cucurbit-associated *F. oxysporum* isolates.

This study investigated the biological differentiation among three cucurbit-associated *F. oxysporum formae speciales* by integrating pathogenicity assays, tissue colonization analyses, and molecular characterization. Pathogenicity and systemic tissue colonization were evaluated under different host species, plant developmental stages, temperature regimes, and propagation systems to identify biological characteristics associated with pathogenic differentiation. Finally, molecular analyses based on the *SIX6* gene together with hierarchical clustering were used to examine whether molecular differentiation was consistent with the biological relationships inferred from pathogenicity and tissue colonization

Results

Baseline pathogenicity of *Fusarium oxysporum* isolates on cucurbit hosts

Baseline pathogenicity was evaluated by root-dip inoculation using nine *Fusarium oxysporum* isolates representing three cucurbit-associated *formae speciales* and nine cultivars from sponge gourd, cucumber, and bitter gourd (Table 1). Distinct pathogenicity patterns were observed among host species, cultivars, and isolate origins 14 days after inoculation.

Among the three sponge gourd cultivars, the *Folu* isolates (Fol114, Fol638, Folust, Folusc, Fomhl6, and Fomhl7) caused severe disease, although disease severity varied among cultivars (Fig. 1A). The cultivar ‘Open Pollination’ (OP) consistently exhibited the highest disease indices and was also susceptible to cross-pathogenic isolates. In addition to the pathogenic *Folu* isolates, the cucumber isolate Foc0812 and the bitter gourd isolates Fomo33 and Fomo35 induced mild disease on OP, with disease indices ranging from 1.50 to 1.67. The Folust isolate recovered from a sponge gourd rootstock and the Folusc, Fomhl6, and Fomhl7 isolates recovered from bitter gourd scions remained pathogenic to sponge gourd, although virulence differed among cultivars.

In cucumber, the cucumber isolate Foc0812 caused the highest disease severity in all three cultivars (Fig. 1B). Several *Folu* isolates (Fol114, Fol638, Folust, Folusc, Fomhl6, and Fomhl7) produced only mild symptoms, indicating limited cross-pathogenicity from sponge gourd to cucumber. Among the

tested cultivars, ‘Vantage’ (VT) was the most susceptible, with disease indices ranging from 0.28 to 1.10 following inoculation with these cross-pathogenic isolates.

In bitter gourd, disease developed only after inoculation with the bitter gourd isolates Fomo33 and Fomo35 across all three tested cultivars, whereas no symptoms were observed following inoculation with the *Folu* or *Foc* isolates (Fig. 1C), indicating a comparatively narrow host range for the *Fomo* isolates under the experimental conditions.

Principal component analysis (PCA) based on disease indices across the nine cucurbit cultivars showed that PC1 and PC2 explained 54.98% and 40.45% of the total variation, respectively (Fig. 1D). The nine *F. oxysporum* isolates formed three distinct clusters according to their pathogenicity profiles across the tested cultivars. The PCA, together with the pathogenicity data, indicated limited cross-pathogenicity between *Folu* and *Foc* on sponge gourd and cucumber, with sponge gourd OP and cucumber VT showing the greatest susceptibility to isolates originating from the alternate host. In contrast, the *Fomo* isolates remained highly host-specific, with cross-pathogenicity detected only on sponge gourd OP (Fig. 1D).

Based on the baseline pathogenicity responses and PCA grouping, five representative isolates (Foc0812, Fol114, Folust, Fomhl6 and Fomo33) were selected for subsequent investigations. Sponge gourd OP and cucumber VT, which exhibited the highest susceptibility to cross-pathogenic isolates, were used as the comparative experimental system for evaluating the effects of host species, temperature, plant growth stage, and tissue colonization. Meanwhile, the commercially important bitter gourd–sponge gourd grafting system was used to investigate pathogen invasion across the graft union in a commercially relevant production system.

Disease development and differential tissue colonization under soil infestation

To determine whether the cross-pathogenicity observed in the baseline root-dip assay could also be established through natural root invasion, five representative *F. oxysporum* isolates (Fol114, Folust, Fomhl6, Foc0812, and Fomo33) were evaluated by soil infestation using sponge gourd OP and cucumber VT. Fourteen days after inoculation, the disease indices **of** sponge gourd seedlings inoculated with Fol114, Folust, Fomhl6, Foc0812, and Fomo33 were 2.9, 2.6, 1.5, 0.0, and 0.7, respectively. The sponge gourd-associated isolates Fol114 and Folust induced significantly higher disease indices than Foc0812 and Fomo33 ($P \leq 0.05$), whereas Fomhl6 exhibited intermediate virulence and differed significantly only from Foc0812. In cucumber, the cucumber-associated isolate Foc0812 caused the highest disease index (DI = 2.6), which was significantly greater than those of the other isolates ($P \leq 0.05$) (Table 2).

Tissue colonization following soil infestation was evaluated by pathogen re-isolation from infected seedlings. In sponge gourd, Fol114, Folust, and Fomhl6 were recovered from the epicotyl with isolation rates of 77.8%, 66.7%, and 44.4%, respectively. Foc0812 was recovered only from the roots (22.2%), whereas Fomo33 was not recovered from any sponge gourd tissues (Fig. 2A). In cucumber, Foc0812

was consistently recovered from all sampled tissues, including the epicotyl (33.3%). In contrast, Fol114 and Folust were recovered from the roots (100.0% and 88.9%, respectively) and hypocotyls (66.7% for both) but failed to colonize the cotyledonary node or epicotyl. Fomo33 was only rarely recovered from the roots and hypocotyls, whereas Fomhl6 was not detected in any cucumber tissue (Fig. 2B).

Effects of temperature and host growth stage on disease development and tissue colonization

Representative isolates were evaluated under two temperature regimes (20 and 28 °C) and at two host growth stages (BBCH-10 and -12). Disease index and tissue colonization were evaluated in sponge gourd OP and cucumber VT 14 days after inoculation.

Disease responses varied with temperature, although the predominant host association of the isolates remained evident (Fig. 3A–D). At 20 °C, the three *Folu* isolates caused severe disease in sponge gourd, whereas Foc0812 caused the greatest disease severity in cucumber. At 28 °C, Fol114 and Folust remained pathogenic to sponge gourd, although disease severity caused by Folust was reduced, and Fomhl6 no longer produced visible symptoms. Foc0812 remained the most pathogenic isolate on cucumber at 28 °C, while Fol114 and Folust caused only mild disease. Similar host-associated patterns were observed at both plant growth stages (Fig. 3E–H). The three *Folu* isolates caused severe disease in sponge gourd at both BBCH-10 and BBCH-12, whereas Foc0812 consistently caused the highest disease severity in cucumber. The remaining isolate–host combinations generally resulted in mild or no symptoms. Thus, temperature and plant growth stage affected the magnitude of disease expression in an isolate-dependent manner but did not substantially alter the predominant host preference of the isolates.

Tissue colonization under the two temperature regimes generally corresponded with the observed disease responses (Fig. 4). In sponge gourd, the Folu isolates were recovered at high frequencies from both the hypocotyl and epicotyl at 20 and 28 °C, indicating consistent upward colonization. Foc0812 and Fomo33 showed lower and more variable recovery from sponge gourd tissues, particularly from the epicotyl. In cucumber, Foc0812 was consistently recovered from both tissues at both temperatures, including a 66.7% recovery frequency from the epicotyl. At 20 °C, the other isolates were absent or recovered only at low frequency from cucumber tissues. At 28 °C, Fol114 and Fomhl6 were recovered at low frequencies exclusively from the hypocotyl, while Folust and Fomo33 were not detected in any cucumber tissues, indicating that the higher temperature further restricted the upward vascular invasion of these non-host isolates into the epicotyl.

Colonization patterns at the two plant growth stages were similarly associated with isolate–host combinations (Fig. 5). In sponge gourd, the *Folu* isolates were consistently recovered from both the hypocotyl and epicotyl at BBCH-10 and BBCH-12. Foc0812 and Fomo33 also colonized sponge gourd tissues under some conditions, but their recovery frequencies were generally more variable, and upward colonization by Fomo33 was not detected at BBCH-12. In cucumber, Foc0812 was consistently

recovered from both the hypocotyl and epicotyl at both growth stages. By contrast, the *Folu* isolates were recovered primarily from the hypocotyl or at relatively low frequencies from the epicotyl, while Fomo33 was not recovered from cucumber tissues. These findings indicate that plant growth stage influenced the frequency and extent of tissue colonization but did not fundamentally change the characteristic colonization behavior of the isolates.

Effects of grafting on disease development and tissue colonization

To determine whether representative *Fusarium oxysporum* isolates could systemically colonize bitter gourd scions through the graft union, grafted seedlings (bitter gourd scion 'Moon Shine' (MS) on sponge gourd rootstock OP) were challenged by soil infestation using representative *Folu* and *Fomo* isolates individually or in combination. Self-rooted sponge gourd seedlings were included as a reference system.

Disease severity differed among isolates but showed similar trends in both grafted and self-rooted seedlings (Table 3). In grafted seedlings, Fol114 caused the most severe disease (DI = 2.00), followed by Fomhl6 (DI = 1.50) and Folust (DI = 1.00), whereas Fomo33 and the mixed-inoculation treatments produced significantly lower disease severity. Likewise, in self-rooted sponge gourd seedlings, the three *Folu* isolates caused significantly greater disease than Fomo33 and the mixed-inoculation treatments, with disease indices ranging from 1.50 to 1.75. Co-inoculation with *Folu* and *Fomo* isolates did not substantially alter disease severity compared with inoculation with the corresponding Folu isolate alone.

The tissue colonization patterns closely reflected the disease responses observed in both grafted and self-rooted seedlings (Fig. 6). In grafted seedlings, Fol114 and Folust were frequently recovered from the bitter gourd epicotyl, with recovery frequencies of 50.0% and 75.0%, respectively, whereas Fomhl6 and Fomo33 were not recovered from the bitter gourd epicotyl following single inoculation (Fig. 6A). In self-rooted sponge gourd seedlings, the three *Folu* isolates were consistently recovered from the hypocotyl (75.0–100.0%), and Fol114 exhibited the highest epicotyl recovery frequency (62.5%), followed by Folust (37.5%) and Fomhl6 (12.5%) (Fig. 6B). In contrast, epicotyl recovery of Fomo33 was not detected in either grafted or self-rooted seedlings. These results demonstrate that Fol114 and Folust were capable of systemic colonization across the graft union into bitter gourd scions, whereas Fomhl6 and Fomo33 exhibited little or no upward movement beyond the rootstock.

Mixed inoculation did not substantially alter the tissue colonization patterns observed following single inoculation (Fig. 6). Both Fol114 + Fomo33 and Folust + Fomo33 treatments resulted in 100.0% recovery from the hypocotyl in both grafted and self-rooted seedlings. However, recovery from the epicotyl remained limited, with recovery frequencies of 0.0 and 12.5% in grafted seedlings and 25.0% for both treatments in self-rooted seedlings (Fig. 6). Isolate-specific PCR further confirmed that the limited recovery observed in mixed inoculations was predominantly attributable to the Folu isolates, whereas Fomo33 exhibited only limited colonization (Table 3).

Integrated analysis of pathogenic behavior across experimental variables

To integrate the disease severity and tissue colonization responses obtained throughout this study, heatmap visualization and hierarchical cluster analysis were performed using an integrated matrix comprising 24 experimental variables derived from different host species, temperature regimes, plant growth stages, and grafting conditions. The heatmap revealed distinct response profiles among the five representative *F. oxysporum* isolates across the experimental variables (Fig. 7A). Fol114, Folust, and Fomhl6 exhibited broadly similar profiles, characterized by strong responses in sponge gourd-related variables, whereas Foc0812 and Fomo33 showed distinct profiles associated primarily with cucumber and bitter gourd, respectively.

Hierarchical clustering separated the five isolates into three major groups corresponding to their original host associations (Fig. 7B). Fol114, Folust, and Fomhl6 formed a single cluster comprising the sponge gourd-associated isolates, whereas Foc0812 and Fomo33 each formed an independent cluster corresponding to the cucumber- and bitter gourd-associated isolates, respectively. This grouping was consistent with the host-specific disease severity and tissue colonization characteristics observed across the preceding experiments.

Evaluation of molecular markers for differentiating cucurbit-associated *Fusarium oxysporum* isolates

To evaluate the ability of different molecular markers to differentiate cucurbit-associated *F. oxysporum* isolates, phylogenetic analyses were first performed using the conventional loci rDNA intergenic spacer (IGS) and *translation elongation factor 1-alpha* (*EF-1α*). The resulting sequences were compared with representative reference sequences retrieved from the National Center for Biotechnology Information (NCBI) database (Table 4). Phylogenetic analyses based on both IGS and *EF-1α* provided limited resolution for differentiating cucurbit-associated *F. oxysporum* isolates (Figs. 8). In both phylogenetic trees, isolates representing different *formae speciales* were frequently grouped together, whereas others formed separate clades irrespective of their host associations. Notably, while Foc0812 clustered alongside reference *F. oxysporum* f. sp. *cucumerinum* isolates in the IGS phylogeny (Fig. 8A), it failed to group with these reference isolates in the *EF-1α* analysis (Fig. 8B), indicating that these conventional loci were insufficient for consistently resolving the biological groupings of cucurbit-associated isolates.

In contrast, phylogenetic analysis based on *SIX6* sequences provided greater phylogenetic resolution than the IGS and *EF-1α* markers (Fig. 9). A single amplicon of approximately 611 bp was consistently amplified from all *Folu* isolates. All *Folu* isolates formed a single subclade with 71% bootstrap support. Among the *Foc* isolates, Foc0812 and Foc127 clustered together with reference *F. oxysporum* f. sp. *cucumerinum* isolates in a well-supported subclade (94% bootstrap support), whereas Foc100 was positioned as a separate lineage basal to both the *F. oxysporum* f. sp. *cucumerinum* and *F. oxysporum* f.

sp. *pisi* subclades. Although the *Fomo* isolates were positioned on the same branch, they did not form a distinct subclade. Overall, compared with the IGS and *EF-1α* markers, the *SIX6* marker provided improved discrimination among the representative cucurbit-associated isolates and produced a phylogenetic topology that was largely consistent with the biological groupings inferred from the pathogenicity, tissue colonization, and hierarchical clustering analyses.

Discussion

This study indicated that cucurbit-associated *Fusarium oxysporum formae speciales* exhibit conditional cross-pathogenicity rather than being strictly restricted to their original hosts. Across the experimental systems evaluated, isolates capable of inducing visible wilt or foliar yellowing symptoms in non-original hosts were consistently recovered beyond the cotyledonary node, whereas weakly pathogenic or non-pathogenic interactions were predominantly associated with colonization confined to the hypocotyl. These observations suggest that successful disease development is closely associated with the ability of the pathogen to achieve systemic tissue colonization. In susceptible hosts, *F. oxysporum* typically spreads through the xylem via microconidia, whereas in resistant or non-host interactions, microconidial proliferation and subsequent systemic movement are often restricted. Similar observations have been reported in common bean, where *F. oxysporum* f. sp. *phaseoli* exhibited 29- to 235-fold greater colonization frequencies in the epicotyls of susceptible cultivars than in resistant cultivars (Garcés-Fiallos et al. 2017). Likewise, García-Sánchez et al. (2010) reported that increased fungal virulence was associated with enhanced vascular colonization. Collectively, these findings highlight systemic tissue colonization beyond the cotyledonary node as a potential biological characteristic associated with pathogenic differentiation among cucurbit-associated *F. oxysporum* isolates.

Among the cultivars examined, sponge gourd cv. ‘Open Pollination’ (OP) exhibited the broadest susceptibility spectrum and supported hypocotyl and epicotyl colonization by all three cucurbit-associated *Fusarium oxysporum formae speciales* under multiple experimental conditions. In contrast, although Folu isolates were capable of infecting cucumber and bitter gourd, disease severity remained host-dependent and reflected the biological differentiation among the three *formae speciales*. Similar observations were reported by Cafri et al. (2005), who showed that *F. oxysporum* f. sp. *cucumerinum* caused only mild symptoms on muskmelon compared with the native muskmelon pathogen, *F. oxysporum* f. sp. *melonis*. These findings also have practical implications for the use of sponge gourd as a rootstock for bitter gourd production in Taiwan. Because cross-pathogenicity was observed among the three cucurbit-associated *F. oxysporum formae speciales*, resistance evaluation of sponge gourd rootstocks should not be based solely on *F. oxysporum* f. sp. *luffae*. Instead, resistance screening against multiple cucurbit-associated *formae speciales* may provide a more comprehensive assessment of rootstock performance under field conditions.

Soil infestation provides a more stringent assessment of host–pathogen compatibility than root-dip inoculation because successful infection requires the pathogen to complete the entire natural infection process before reaching host tissues (Gerlagh and Blok 1988). Under these conditions, cucumber VT

developed mild stunting following inoculation with Folust in addition to Foc0812, demonstrating that certain *Folu* isolates retained the ability to establish infection in cucumber through natural root invasion. In contrast, although Fomo33 induced slight growth suppression in sponge gourd OP, the pathogen was not recovered from any plant tissue. This discrepancy suggests that visible growth reduction alone may not necessarily indicate successful host colonization and highlights the importance of combining symptom assessment with pathogen re-isolation to distinguish successful colonization from symptom development in the absence of detectable pathogen establishment during the evaluation of cross-pathogenicity.

Temperature substantially modified the expression of cross-pathogenicity among the cucurbit-associated *F. oxysporum formae speciales*. Although several isolates remained capable of infecting their preferred hosts under suboptimal temperatures, disease severity was generally reduced. Similar temperature-dependent pathogenicity has been reported for *F. oxysporum* f. sp. *radicis-cucumerinum*, which causes severe disease under cool conditions (17–23°C) but not above 29°C (Vakalounakis, 1996). In the present study, the *Folu* isolate Fomhl6 failed to induce visible symptoms in sponge gourd at 28°C despite successful colonization beyond the cotyledonary node, suggesting that latent systemic colonization can occur under unfavorable temperature regimes. Similar symptomless systemic colonization has been documented in several crops infected by *F. oxysporum*, suggesting that symptomless hosts may serve as pathogen reservoirs within production systems (Chen et al. 2023; Malcolm et al. 2013). In contrast, *Fomo* isolate Fomo33 failed to infect sponge gourd at 20°C but induced disease symptoms at 28°C, consistent with previous findings that elevated temperatures may suppress host resistance mechanisms (Webb et al. 2015). Although *Luffa* spp. and *Cucurbita* spp. have previously been regarded as non-hosts for *Fomo* (Cumagun et al. 2010), the results suggest that sponge gourd may function as an alternative host species under high-temperature conditions.

Host developmental stage also influenced the expression of cross-pathogenicity. Seedlings inoculated at the cotyledon stage (BBCH-10) were generally more susceptible than those inoculated at the second true leaf stage (BBCH-12), consistent with previous reports that young seedlings are more vulnerable to *Fusarium oxysporum* infection (Rispail et al. 2015). As plants develop, structural barriers and inducible defense responses generally become more effective, thereby reducing disease susceptibility (Nyvall and Haglund, 1976). This developmental difference was also reflected in the tissue colonization patterns observed in the present study, further supporting the influence of host developmental stage on successful pathogen establishment. In addition, because seedlings at BBCH-10 had not yet developed fully expanded true leaves, conventional leaf yellowing-based disease assessments were less suitable, indicating that disease evaluation methods may require refinement for very early-stage infections.

To better simulate natural infection under field conditions, grafted and non-grafted plants were challenged through soil infestation. The grafting experiments demonstrated that pathogen movement across the graft union differed among the cucurbit-associated *Fusarium oxysporum formae speciales*. When inoculated alone, *Fomo* did not induce disease in either self-rooted sponge gourd seedlings or bitter gourd scions grafted onto sponge gourd rootstocks. In contrast, Folu isolates successfully

colonized grafted plants and induced typical wilt symptoms. Furthermore, under co-inoculation conditions, molecular detection consistently identified only *Folu*, but not *Fomo*, in symptomatic epicotyl tissues, suggesting that the sponge gourd rootstock restricted the upward movement of Fomo into the bitter gourd scion under the conditions examined. Whether this phenomenon occurs in other *Luffa* cultivars remains to be investigated.

Interestingly, although Fomo33 was not recovered from self-rooted sponge gourd seedlings, it was detected in the hypocotyls of grafted plants, suggesting that grafting may alter the interaction between the pathogen and the rootstock. Previous studies have shown that grafting modifies root exudate composition and may consequently influence *Fusarium* colonization. For example, grafted watermelon–bottle gourd combinations exhibited weaker antifungal activity in root exudates than bottle gourd plants alone (Ling et al. 2013). Likewise, the interaction between rootstock and scion is bidirectional, and the scion genotype can influence root-mediated defense responses (Cohen et al. 2002). In addition, some *Folu* isolates exhibited limited upward movement and remained confined to the rootstock, which may reflect non-host resistance operating within the bitter gourd scion, as previously reported in melon grafting systems (Cohen et al. 2002; Guan et al. 2012).

The co-inoculation experiments also highlighted an important methodological consideration. Because multiple *Fusarium* isolates were simultaneously introduced into the same plant, colony morphology alone was insufficient to determine whether recovered isolates corresponded to the original inoculated strain. Similar observations have been reported in cucurbit production systems, where non-pathogenic *Fusarium* spp. are frequently recovered from plants grown in non-sterile substrates (Wang et al. 2013). Therefore, forma specialis-specific PCR assays were essential for confirming the identity of recovered isolates and for accurately interpreting pathogen colonization patterns in the co-inoculation experiments.

Phylogenetic analyses based on the conserved IGS and *EF-1α* loci provided limited resolution for differentiating the three cucurbit-associated *Fusarium oxysporum formae speciales*, consistent with previous studies reporting substantial phylogenetic overlap among *formae speciales*, including f. sp. *rapae* or *cepae* (Dissanayake et al. 2009; Enya et al. 2008). In contrast, phylogenetic analysis based on the virulence-associated SIX6 gene provided improved discrimination among the representative cucurbit-associated isolates and was largely congruent with the biological groupings inferred from the pathogenicity, tissue colonization, and hierarchical clustering analyses. This correspondence suggests that pathogenicity-associated effector genes may better reflect the biological differentiation of host-adapted populations than conserved phylogenetic loci. However, because SIX genes have also been identified in non-pathogenic Fusarium isolates (Jelinski et al. 2017), and authenticated *SIX6* sequences of *F. oxysporum* f. sp. *luffae* remain unavailable in public databases, the broader applicability of *SIX6* for differentiating cucurbit-associated *formae speciales* requires further validation using a larger and more geographically diverse collection of isolates.

Beyond the individual experimental observations, a consistent biological pattern emerged throughout this study. Across different host species, temperature regimes, plant developmental stages, and propagation systems, pathogenic differentiation among the selected cucurbit-associated *F. oxysporum* isolates was more closely associated with their ability to achieve systemic tissue colonization than with host origin alone. Although environmental and developmental factors influenced disease severity and pathogen recovery frequency, the characteristic patterns of systemic colonization remained largely consistent among the representative isolates. These findings suggest that the capacity to colonize host tissues beyond the cotyledonary node is a consistent biological characteristic associated with pathogenic differentiation, rather than a context-dependent response to individual experimental conditions. Furthermore, the congruent grouping inferred from *SIX6* sequence analysis provides complementary molecular support for this biological differentiation. Together, these findings demonstrate that integrating biological observations with molecular evidence provides a more comprehensive framework for characterizing pathogenic differentiation among cucurbit-associated *F. oxysporum* isolates.

Conclusion

Collectively, this study demonstrates that biological differentiation among cucurbit-associated *Fusarium oxysporum* formae speciales is consistently supported by pathogenicity, tissue colonization, and molecular evidence. Although cross-pathogenicity was observed among the three *formae speciales*, pathogenic differentiation was more closely associated with the ability to achieve systemic tissue colonization beyond the cotyledonary node than with host origin alone. Phylogenetic analysis based on the *SIX6* gene further provided complementary molecular support for the biologically defined groups identified in this study. Together, these findings improve our understanding of pathogenic differentiation among cucurbit-associated *F. oxysporum* isolates and provide a biological and molecular basis for future studies of host specialization, resistance screening, rootstock evaluation, and disease management in cucurbit production systems.

Materials and Methods

Fungal Isolates and Plant Materials

Nine *Fusarium oxysporum* isolates representing three cucurbit-associated *formae speciales* were included in this study, comprising two *F. oxysporum* f. sp. *luffae* (*Folu*) isolates (Fol114 and Fol638), one *F. oxysporum* f. sp. *cucumerinum* (*Foc*) isolate (Foc0812), and two *F. oxysporum* f. sp. *momordicae* (*Fomo*) isolates (Fomo33 and Fomo35). Additionally, four *Folu* isolates recovered from naturally infected bitter gourd–sponge gourd grafted plants were included, consisting of two isolates from sponge gourd rootstocks (Folust and Folusc) and two isolates from bitter gourd scions (Fomhl6 and Fomhl7). All isolates were initially cultured on 2% water agar (WA) at 28°C under a 12-h photoperiod to induce sporulation. Single-conidial cultures were then transferred to potato dextrose agar (PDA) and incubated under the same conditions for subsequent experiments. Three cucurbit species, namely sponge gourd

(*Luffa cylindrica*), cucumber (*Cucumis sativus*), and bitter gourd (*Momordica charantia*), were used throughout this study. Detailed information on all fungal isolates and the plant cultivars used in each experiment is provided in Table 1.

General Inoculation Procedures and Tissue Re-isolation

Two inoculation methods were employed throughout this study. Root-dip inoculation was used for baseline pathogenicity assays, whereas soil infestation was used to evaluate natural infection, tissue colonization, and subsequent environmental and grafting experiments.

For root-dip inoculation, conidial suspensions were prepared at a concentration of 1×10^6 conidia mL^{-1}. Except for the plant growth-stage experiment, seedlings were washed to remove the rhizosphere substrate, immersed in the conidial suspension for 30 min, and transplanted into 13 × 13 cm pots containing peat moss. Each treatment consisted of ten plants with two biological replicates, and non-inoculated plants served as controls.

For soil infestation, *F. oxysporum* isolates were cultured on potato dextrose agar (PDA) at 28°C under a 12-h photoperiod for 7 days. Fungal inoculum was prepared using a sterilized oat grain–sand substrate (oat grain : sand : sterile distilled water = 100:100:20, w/w/v) and incubated at room temperature (25–30°C) until the substrate was fully colonized. The inoculum was homogenized using an RT-04 homogenizer (Rong Tsong Co., Ltd., Taichung, Taiwan) and mixed with sterile soil to obtain a final concentration of 5×10^3 propagules g^{-1} soil. Seedlings were transplanted into 8 × 9 cm pots containing the infested soil, whereas seedlings grown in pathogen-free peat moss served as non-inoculated controls.

Disease severity was evaluated at the designated assessment time for each experiment using a 0–4 disease index (DI) scale: 0 = no symptoms; 1 = stunting or initial chlorosis; 2 = ≤ 50% leaf yellowing; 3 = > 50% leaf yellowing; and 4 = wilting or plant death.

Following disease assessment, representative plants were sampled for tissue re-isolation. Surface sterilization was performed by sequential immersion in a mixture of 95% ethanol and 6.25% sodium hypochlorite (1:1, v/v) for approximately 15 s, followed by immersion in 75% ethanol. The tissues were rinsed three times with sterile distilled water, dried on sterile paper towels, cut into appropriate sizes, and placed on pentachloronitrobenzene (PCNB) medium. Plates were incubated at 28°C for 7 days and examined for fungal colonies emerging from the vascular cut surfaces. Colony morphology was recorded, and recovered *Fusarium* isolates were further confirmed using forma specialis-specific PCR assays when necessary, particularly for experiments involving mixed inoculations. The sampling strategy and tissues examined varied according to the objectives of each experiment and are described in the corresponding sections below.

Experimental design for pathogenicity and tissue colonization assays

Baseline pathogenicity assays

Baseline pathogenicity assays were conducted using nine cultivars representing three major cucurbit species: cucumber (*Cucumis sativus*) [cvs. ‘Pretty Swallow’ (PS), ‘Shiou-leu’ (SL), and ‘Vantage’ (VT)]; sponge gourd (*Luffa cylindrica*) [cvs. ‘A-shuenn No.1’ (AS1), ‘Merit’ (MT), and ‘Open Pollination’ (OP)]; and bitter gourd (*Momordica charantia*) [cvs. ‘Moon Shine’ (MS), ‘Verdant’ (VD), and ‘Yingzui’ (YZ)]. Seeds were soaked in tap water for 24 h to promote germination and sown in 36-cell plug trays (5 × 5 × 5 cm) containing peat moss. Seedlings were grown in a greenhouse at 25–28°C and inoculated using the root-dip procedure described above. Disease severity was assessed 14 days after inoculation.

Disease development and tissue colonization under soil infestation

Representative isolates, including three *Folu* isolates (Fol114, Folust, and Fomhl6), one *Foc* isolate (Foc0812), and one *Fomo* isolate (Fomo33), were selected based on the baseline pathogenicity assays. Sponge gourd cv. 'Open Pollination' (OP) and cucumber cv. 'Vantage' (VT), which exhibited high susceptibility in the baseline pathogenicity assays, were selected as host plants. Seedlings were grown in a greenhouse at 25–28°C and inoculated using the soil infestation procedure described above.

Disease severity was assessed 14 days after inoculation. To evaluate tissue colonization, pathogen re-isolation was conducted from the roots, hypocotyls, cotyledonary nodes, and epicotyls. In addition, the infested soil associated with each plant was sampled to determine the persistence of *F. oxysporum* using PCNB medium. Each experimental unit consisted of one pot representing a single biological replicate for pathogen isolation, and the entire experiment was conducted twice.

Evaluation of thermal regimes and ontogenetic stages on disease dynamics

The effects of temperature and host growth stage on pathogenicity and tissue colonization were evaluated using five representative *Fusarium oxysporum* isolates (Fol114, Folust, Fomhl6, Foc0812, and Fomo33) and two susceptible host cultivars, sponge gourd cv. 'Open Pollination' (OP) and cucumber cv. 'Vantage' (VT).

For temperature experiments, seedlings were inoculated using the root-dip procedure described above and incubated at either 20 or 28°C under a 12-h photoperiod. Disease severity and tissue colonization were evaluated 14 days after inoculation. The entire experiment was conducted twice

For host growth-stage experiments, two developmental stages were evaluated: cotyledons completely unfolded (BBCH growth stage 10) and second true leaf unfolded (BBCH growth stage 12). Seedlings were inoculated using the same root-dip procedure and incubated at 20°C under a 12-h photoperiod. Disease severity and tissue colonization were evaluated 14 days after inoculation. The entire experiment was conducted twice

.

Grafting assay and dual-isolate co-inoculation regimes

To evaluate pathogen colonization across the graft union under conditions simulating natural infection, bitter gourd scions grafted onto sponge gourd rootstocks were challenged using the soil infestation procedure described above. Bitter gourd MS was used as the scion, whereas sponge gourd OP served as the rootstock. Grafted seedlings were inoculated one week after grafting.

Four representative *F. oxysporum* isolates, including three *Folu* isolates (Fol114, Folust, and Fomhl6) and one *Fomo* isolate (Fomo33), were used to establish seven inoculation treatments: Fol114, Folust, Fomhl6, Fomo33, Fol114 + Fomo33, Folust + Fomo33, and Fomhl6 + Fomo33. Grafted seedlings were transplanted into 13 × 13 cm pots containing infested soil and maintained in a growth chamber at 20°C under a 12-h photoperiod. Disease severity and tissue colonization were evaluated four weeks after inoculation.

Because two *formae speciales* were simultaneously introduced in the mixed-inoculation treatments, colony morphology alone was insufficient to determine the identity of recovered isolates. Therefore, recovered *Fusarium* isolates were further identified using forma specialis-specific PCR assays. Following tissue re-isolation, plants were separated into roots, hypocotyls, cotyledonary nodes, and stems, and approximately 0.1 g of tissue from each section was collected for DNA extraction. Genomic DNA was extracted using a Plant Genomic DNA Purification Kit (Genemark Technology Co., Ltd., Taichung, Taiwan). DNA quality was first verified using the universal fungal primer pair ITS1 (5'-TCCGTAGGTGAACCTGCGG-3') and ITS4 (5'-TCCTCCGCTTATTGATATGC-3') (White et al. 1990). PCR amplification was performed in a 25-μL reaction containing 5 μL PCR Master Mix (Genemark Technology Co., Ltd., Taichung, Taiwan), 0.5 μL of each primer (10 μM), 1 μL template DNA, and nuclease-free water. Thermal cycling consisted of an initial denaturation at 95°C for 2 min, followed by 35 cycles of 95°C for 30 s, 55°C for 30 s, and 72°C for 2 min, with a final extension at 72°C for 5 min.

Forma specialis-specific PCR assays were subsequently performed using primers reported by van Dam et al. (2018). Primer pair fp7320/fp7337 was used to detect Folu, whereas primer pair fp7318/fp7335 was used to detect Fomo. PCR reactions were performed in 25-μL volumes using the same reaction mixture described above. Thermal cycling conditions for the Folu-specific primers consisted of 94°C for 2 min; 35 cycles of 94°C for 30 s, 54°C for 30 s, and 72°C for 40 s; followed by a final extension at 72°C for 5 min. For the Fomo-specific primers, the annealing temperature was changed to 60°C, whereas all other cycling conditions remained identical. PCR products were analyzed by agarose gel electrophoresis to determine the distribution of Folu and Fomo within grafted plant tissues.

Integrated analysis of pathogenic behavior across experimental variables

Disease indices within each experiment were analyzed using one-way analysis of variance (ANOVA), followed by Tukey's honestly significant difference (HSD) test at $p \leq 0.05$. Statistical analyses were

performed using IBM SPSS Statistics version 20 (IBM Corp., Armonk, NY, USA).

Principal component analysis (PCA) was performed using the baseline pathogenicity data obtained from all isolate–host combinations to evaluate relationships among *F. oxysporum* isolates based on host responses.

To integrate pathogenicity and tissue colonization data obtained under different experimental conditions, hierarchical clustering and heatmap analyses were performed using the five representative isolates evaluated in this study. Twenty-four variables, including disease indices and tissue colonization frequencies under different host species, temperature regimes, plant growth stages, and grafting conditions, were included in the analysis. Prior to clustering, all variables were normalized to minimize differences in measurement scales. Hierarchical clustering was performed using Euclidean distance as the similarity metric and Ward's linkage method. Heatmaps and dendrograms were generated to visualize the relationships among isolates across all experimental conditions.

Molecular characterization

DNA extraction

Genomic DNA was extracted once from each *F. oxysporum* isolate included in this study and subsequently used for all downstream PCR amplifications and sequencing analyses. Fungal DNA was extracted from fresh mycelia using a modified protocol based on Saitoh et al. (2006). Briefly, isolates were cultured on potato dextrose agar (PDA) at 28°C under a 12-h photoperiod for 5–7 days. Fresh mycelia were harvested and lysed in an extraction buffer consisting of 200 mM Tris-HCl, 50 mM EDTA, 200 mM NaCl, and 1% sodium *N*-lauroylsarcosinate (pH 8.0), followed by phenol–chloroform extraction and isopropanol precipitation. DNA pellets were washed twice with 70% ethanol, air-dried, resuspended in 30 µL of ultrapure water, incubated at 55°C for 20 min, and stored at − 20°C until further use.

PCR amplification and sequencing

The rDNA intergenic spacer (IGS), *translation elongation factor 1-alpha* (*EF-1α*), and *Secreted in Xylem 6* (*SIX6*) regions were amplified by PCR using published primer pairs. Unless otherwise stated, PCR was performed in a 25-µL reaction containing 5 µL PCR Master Mix (Genemark Technology Co., Ltd., Taichung, Taiwan), 0.5 µL of each primer (10 µM), 1 µL template DNA, and nuclease-free water to a final volume. The rDNA IGS region was amplified using primer pair CNL12/CNS1(5’-CTGAACGCCTCTAAGTCAG-3’/5’-GAGACAAGCATATGACTACTG-3’) (Appel and Gordon, 1995), whereas *EF-1α* was amplified using primer pair EF-1H/EF-2T (5’-ATGGGTAAGGAAGACAAGAC-3’/5’-GGAAGTACCAGTGATCATGTT-3’) (O'Donnell et al. 1998). Both loci were amplified using identical cycling conditions consisting of an initial denaturation at 94°C for 10 min, followed by 35 cycles of 94°C for 1 min, 60°C for 1.5 min, and 72°C for 2 min. The SIX6 gene was amplified using primer pair SIX6-F/SIX6-R (5’-GGCTGCGTAGCTGGTCCCCT-3’/5’-CATGTCATGAATGTACGCATGTCCCT-3’) (Meldrum et al. 2012). PCR amplification consisted of an initial denaturation at 94°C for 10 min, followed by 35 cycles of 94°C for 45 s, 60°C for 45 s, and 72°C for 1 min, with a final extension at 72°C for 10 min.

Phylogenetic analysis

Phylogenetic analyses were performed using the Maximum Likelihood (ML) method implemented in MEGA version 11 (Tamura et al. 2021) under the Tamura–Nei substitution model. Branch support was evaluated with 1,000 bootstrap replicates, and alignment gaps were excluded from all analyses. Representative *F. oxysporum* sequences retrieved from GenBank were included as reference isolates for phylogenetic comparison.

Declarations

Data availability

All data has been provided with the manuscript.

Author information

Authors and Affiliations

1. **Department of Plant Medicine, National Chiayi University, Chiayi City, 600, Taiwan**

Yi-Jeng Chen

2. **Taichung District Agricultural Research and Extension Station, MOA, Changhua County, 515, Taiwan**

Chao-Jen Wang

3. **Department of Plant Pathology, National Chung Hsing University, Taichung, 402, Taiwan**

Ching-Chen Chung & Wen-Hsin Chung

4. **Master Program in Plant Medicine and Good Agricultural Practice, National Chung Hsing University, Taichung, 402, Taiwan**

Wen-Hsin Chung

Contributions

All authors contributed to the study conception and design. Wen-Hsin Chung and Yi-Jeng Chen conceived and designed the experiments. Chao-Jen Wang prepared the primary materials and provided

the fungal isolates used in this study. Ching-Chen Chung conducted most of the experiments. Yi-Jeng Chen analyzed the data. Yi-Jeng Chen and Ching-Chen Chung drafted the manuscript. Wen-Hsin Chung revised the manuscript. All authors read and approved the final manuscript.

Corresponding authors

Correspondence to Wen-Hsin Chung; E-mail: wenchung@nchu.edu.tw; Tel: +886-2284-0356#354

Ethics declarations

Ethics approval and consent to participate

Not applicable.

Consent for publication

All authors have approved the manuscript and agree with its publication.

Competing interests

The authors declare that they have no competing interests.

Tables

Tables 1-4 are available in the Supplementary Files section.

References

1. Alkher H, El Hadrami A, Rashid K, Adam L, Daayf F (2009) Cross-pathogenicity of *Verticillium dahliae* between potato and sunflower. Eur J Plant Pathol 124:505–519. 10.1007/s10658-009-9437-z
2. Armstrong GM, Armstrong JK (1978) Formae speciales and races of *Fusarium oxysporum* causing wilts of the Cucurbitaceae. Phytopathology 68:19–28. 10.1094/Phyto-68-19
3. Appel DJ, Gordon TR (1995) Intraspecific variation within populations of *Fusarium oxysporum* based on RFLP analysis of the intergenic spacer region of the rDNA. Exp Mycol 19:120–128. 10.1006/emyc.1995.1014
4. Cafri D, Katan J, Katan T (2005) Cross-pathogenicity between formae speciales of *Fusarium oxysporum*, the pathogens of cucumber and melon. J Phytopathol 153:615–622. 10.1111/j.1439-0434.2005.01029.x

5. Chen YJ, Chen HJ, Chung WH (2023) Endophytic fungal diversity in *Cirsium kawakamii* from Taiwan. J Fungi 9:1076. 10.3390/jof9111076
6. Cohen R, Horev C, Burger Y, Shriber S, Hershenhorn J, Katan J, Edelstein M (2002) Horticultural and pathological aspects of Fusarium wilt management using grafted melons. HortScience 37:1069–1073
7. Cohen R, Orgil G, Burger Y, Saar U, Elkabetz M, Tadmor Y et al (2015) Differences in the responses of melon accessions to *Fusarium oxysporum* f. sp. *radicis-cucumerinum* and their colonization by the pathogen. Plant Pathol 64:655–663. 10.1111/ppa.12286
8. Correll JC (1991) The relationship between *formae speciales*, races, and vegetative compatibility groups in *Fusarium oxysporum*. Phytopathology 81:1061–1064
9. Cumagun CJR, Aguirre JA, Relevante CA, Balatero CH (2010) Pathogenicity and aggressiveness of *Fusarium oxysporum* Schl. in bottle gourd and bitter gourd. Plant Protect Sci 46:51–58. 10.17221/18/2009-PPS
10. Dissanayake MLMC, Kashima R, Tanaka S, Ito S-I (2009) Genetic diversity and pathogenicity of *Fusarium oxysporum* isolated from wilted Welsh onion in Japan. J Gen Plant Pathol 75:125–130. 10.1007/s10327-009-0152-6
11. Edel-Hermann V, Lecomte C (2019) Current status of *Fusarium oxysporum* formae speciales and races. Phytopathology 109:512–530. 10.1094/PHYTO-08-18-0320-RVW
12. Enya J, Togawa M, Takeuchi T, Yoshida S, Tsushima S, Arie T et al (2008) Biological and phylogenetic characterization of the *Fusarium oxysporum* species complex causing yellows on *Brassica* spp., and proposal of *Fusarium oxysporum* f. sp. *rapae*, a novel *forma specialis* pathogenic on *Brassica rapa* in Japan. Phytopathology 98:475–483. 10.1094/PHYTO-98-4-0475
13. Fraser-Smith S, Czislowski E, Meldrum RA, Zander M, O'Neill W, Balali GR, Aitken EAB (2014) Sequence variation in the putative effector gene SIX8 facilitates molecular differentiation of *Fusarium oxysporum* f. sp. *cubense*. Plant Pathol 63:1044–1052. 10.1111/ppa.12184
14. Garcés-Fiallos FR, de Borba MC, Schmidt ÉC, Bouzon ZL, Stadnik MJ (2017) Delayed upward colonization of xylem vessels is associated with resistance of common bean to *Fusarium oxysporum* f. sp. *phaseoli*. Eur J Plant Pathol 149:477–489. 10.1007/s10658-017-1197-6
15. García-Sánchez MA, Martín-Rodrigues N, Ramos B, de Vega-Bartol JJ, Perlin MH, Díaz-Mínguez JM (2010) Fost12, the *Fusarium oxysporum* homolog of the transcription factor Ste12, is upregulated during plant infection and required for virulence. Fungal Genet Biol 47:216–225. 10.1016/j.fgb.2009.11.006
16. Gerlagh M, Blok WJ (1988) *Fusarium oxysporum* f. sp. *cucurbitacearum* f. nov. embracing all *formae speciales* of *Fusarium oxysporum* attacking cucurbitaceous crops. Eur J Plant Pathol 94:17–31. 10.1007/BF01999804
17. Guan W, Zhao X, Hassell R, Thies J (2012) Defense mechanisms involved in disease resistance of grafted vegetables. HortScience 47:164–170. 10.21273/HORTSCI.47.2.164

18. Gwynne BJ, Gordon TR, Davis RM (1997) A new race of *Fusarium oxysporum* f. sp. *melonis* causing Fusarium wilt of muskmelon in the Central Valley of California. Plant Dis 81:1095
19. Jelinski NA, Broz K, Jonkers W, Ma LJ, Kistler HC (2017) Effector gene suites in some soil isolates of *Fusarium oxysporum* are not sufficient predictors of vascular wilt in tomato. Phytopathology 107:842–851. 10.1094/PHYTO-12-16-0437-R
20. Jenkins S, Taylor A, Jackson AC, Armitage AD, Bates HJ, Mead A, Harrison RJ, Clarkson JP (2021) Identification and expression of secreted in xylem pathogenicity genes in *Fusarium oxysporum* f. sp. *pisi*. Front Microbiol 12:593140. 10.3389/fmicb.2021.593140
21. Lievens B, Houterman PM, Rep M (2009) Effector gene screening allows unambiguous identification of *Fusarium oxysporum* f. sp. *lycopersici* races and discrimination from other *formae speciales*. FEMS Microbiol Lett 300:201–215. 10.1111/j.1574-6968.2009.01783.x
22. Lin YS, Chen YJ, Wang CJ (2011) Wilt-type disease of cucurbitaceous plants in field. Available at: http://gimi.tmu.edu.tw/files/archive/33_d83cf40f.pdf (Accessed 15 March 2022)
23. Lin YS, Huang CH, Kuo MS (1996) Occurrence and dissemination of Fusarium wilt of bitter gourd in Taiwan. Plant Pathol Bull 5:38–46. 10.6649/PPB.199603_5(1).0005
24. Ling N, Zhang W, Wang D, Mao J, Huang Q, Guo S, Shen Q (2013) Root exudates from grafted-root watermelon contribute to inhibition of *Fusarium oxysporum* f. sp. *niveum*. PLoS ONE 8:e63383. 10.1371/journal.pone.0063383
25. Malcolm GM, Kuldau GA, Gugino BK, Jiménez-Gasco MDM (2013) Hidden host plant associations of soilborne fungal pathogens: an ecological perspective. Phytopathology 103:538–544. 10.1094/PHYTO-08-12-0192
26. Martyn RD, Bruton BD (1989) An initial survey of the United States for races of *Fusarium oxysporum* f. sp. niveum HortScience 24:696–698. 10.21273/HORTSCI.24.4.696
27. Meldrum RA, Fraser-Smith S, Tran-Nguyen LTT, Daly AM, Aitken EAB (2012) Presence of putative pathogenicity genes in isolates of *Fusarium oxysporum* f. sp. *cubense* from Australia. Austral Plant Pathol 41:551–557. 10.1007/s13313-012-0122-x
28. Nyvall RF, Haglund WA (1976) Effect of plant age on severity of pea wilt caused by *Fusarium oxysporum* f. sp. *pisi* race 5. Phytopathology 66:1093–1096. 10.1094/Phyto-66-1093
29. O'Donnell K, Kistler HC, Cigelnik E, Ploetz RC (1998) Multiple evolutionary origins of the fungus causing Panama disease of banana: concordant evidence from nuclear and mitochondrial gene genealogies. PNAS 95:2044–2049. 10.1073/pnas.95.5.2044
30. Owen JH (1956) Cucumber wilt caused by *Fusarium oxysporum* f. sp. *cucumerinum*. Phytopathology 46:153–157
31. Palti J, Joffe AZ (1971) Causes of the Fusarium wilts of cucurbits in Israel and conditions favoring their development. J Phytopathol 70:31–42. 10.1111/j.1439-0434.1971.tb03460.x
32. Rispail N, Bani M, Rubiales D (2015) Resistance reaction of *Medicago truncatula* genotypes to *Fusarium oxysporum*: effect of plant age, substrate and inoculation method. Crop Pasture Sci 66:506–515. 10.1071/CP14216

33. Saitoh KI, Togashi K, Arie T, Teraoka T (2006) A simple method for a mini-preparation of fungal DNA. J Gen Plant Pathol 72:348–350
34. Tamura K, Stecher G, Kumar S (2021) MEGA11: Molecular Evolutionary Genetics Analysis version 11. Mol Biol Evol 38:3022–3027. 10.1093/molbev/msab120
35. Tuttle McGrath M (2004) Diseases of cucurbits and their management. In: Naqvi SAMH (ed) Diseases of Fruits and Vegetables, vol I. Springer, Dordrecht. doi: 10.1007/1-4020-2606-4_12.
36. Vakalounakis DJ (1996) Root and stem rot of cucumber caused by *Fusarium oxysporum* f. sp. *radicis-cucumerinum* f. sp. nov. Plant Dis 80:313
37. Vakalounakis DJ (1993) Inheritance and genetic linkage of Fusarium wilt (*Fusarium oxysporum* f. sp. *cucumerinum* race 1) and scab (*Cladosporium cucumerinum*) resistance genes in cucumber (*Cucumis sativus*). Ann Appl Biol 123:359–365
38. van Dam P, de Sain M, ter Horst A, van der Gragt M, Rep M (2018) Use of comparative genomics-based markers for discrimination of host specificity in *Fusarium oxysporum*. Appl Environ Microbiol 84:e01868–e01817. 10.1128/AEM.01868-17
39. van Dam P, Fokkens L, Schmidt SM, Linmans JH, Kistler HC, Ma LJ, Rep M (2016) Effector profiles distinguish *formae speciales* of *Fusarium oxysporum*. Environ Microbiol 18:4087–4102. 10.1111/1462-2920.13445
40. Wang CJ, Lin YS, Lin YH, Chung WH (2013) Modified primers for the identification of nonpathogenic *Fusarium oxysporum* isolates that have biological control potential against Fusarium wilt of cucumber in Taiwan. PLoS ONE 8:e65093. 10.1371/journal.pone.0065093
41. Webb KM, Brenner T, Jacobsen BJ (2015) Temperature effects on the interactions of sugar beet with *Fusarium oxysporum* f. sp. *betae*. Can J Plant Pathol 37:353–362
42. White TJ, Bruns T, Lee S, Taylor J (1990) Amplification and direct sequencing of fungal ribosomal RNA genes for phylogenetics. In: Innis MA, Gelfand DH, Sninsky JJ, White TJ (eds) PCR Protocols: A Guide to Methods and Applications. Academic, San Diego, pp 315–322
43. Zhang Y, Yang H, Turra D, Zhou S, Ayhan DH, DeIulio GA, Guo L, Broz K, Wiederhold N, Coleman JJ, Donnell KO, Youngster I, McAdam AJ, Savinov S, Shea T, Young S, Zeng Q, Rep M, Pearlman E, Schwartz DC, Di Pietro A, Kistler HC, Ma LJ (2020) The genome of the opportunistic fungal pathogen *Fusarium oxysporum* carries a unique set of lineage-specific chromosomes. Commun Biol 3:50. 10.1038/s42003-020-0770-2

Figures

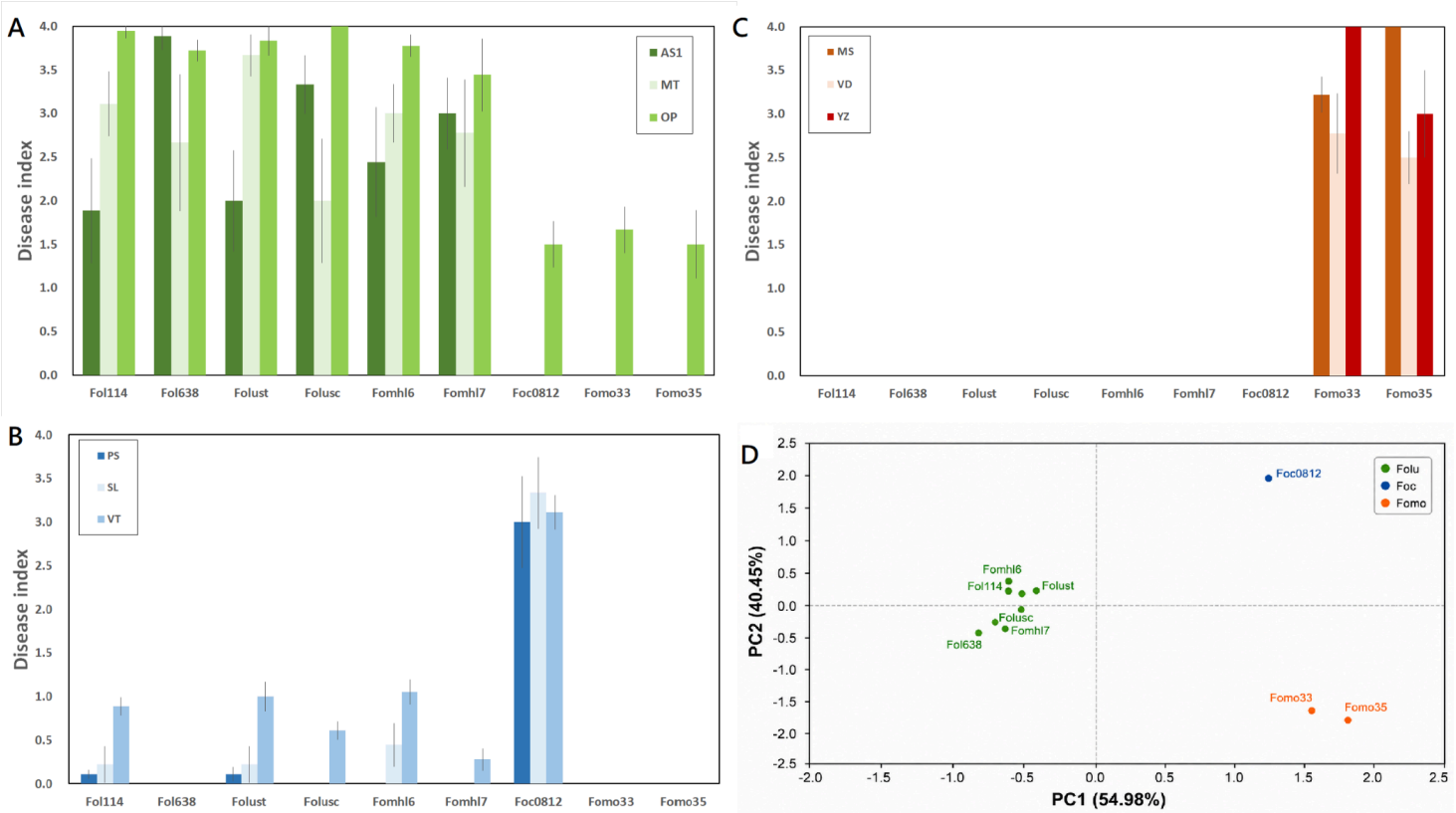


Figure 1

Baseline pathogenicity responses of nine *Fusarium oxysporum* (Fo) isolates on cucurbit hosts and principal component analysis (PCA) of disease severity following root-dip inoculation. Disease indices of three sponge gourd (*Luffa cylindrica*) cultivars, 'A-shuenn No. 1' (AS1), 'Merit' (MT), and 'Open Pollination' (OP), following inoculation with nine Fo isolates (A). Disease indices of three cucumber (*Cucumis sativus*) cultivars, 'Pretty Swallow' (PS), 'Shiou-leu' (SL), and 'Vantage' (VT) (B). Disease indices of three bitter gourd (*Momordica charantia*) cultivars, 'Moon Shine' (MS), 'Verdant' (VD), and 'Yingzui' (YZ) (C). Principal component analysis (PCA) based on disease indices across all nine host cultivars, showing the separation of the nine Fo isolates into three host-associated groups. PC1 and PC2 explained 54.98% and 40.45% of the total variation, respectively (D). Isolates are color-coded according to *forma specialis*: Folu (green), Foc (blue), and Fomo (red). Error bars represent standard deviations.

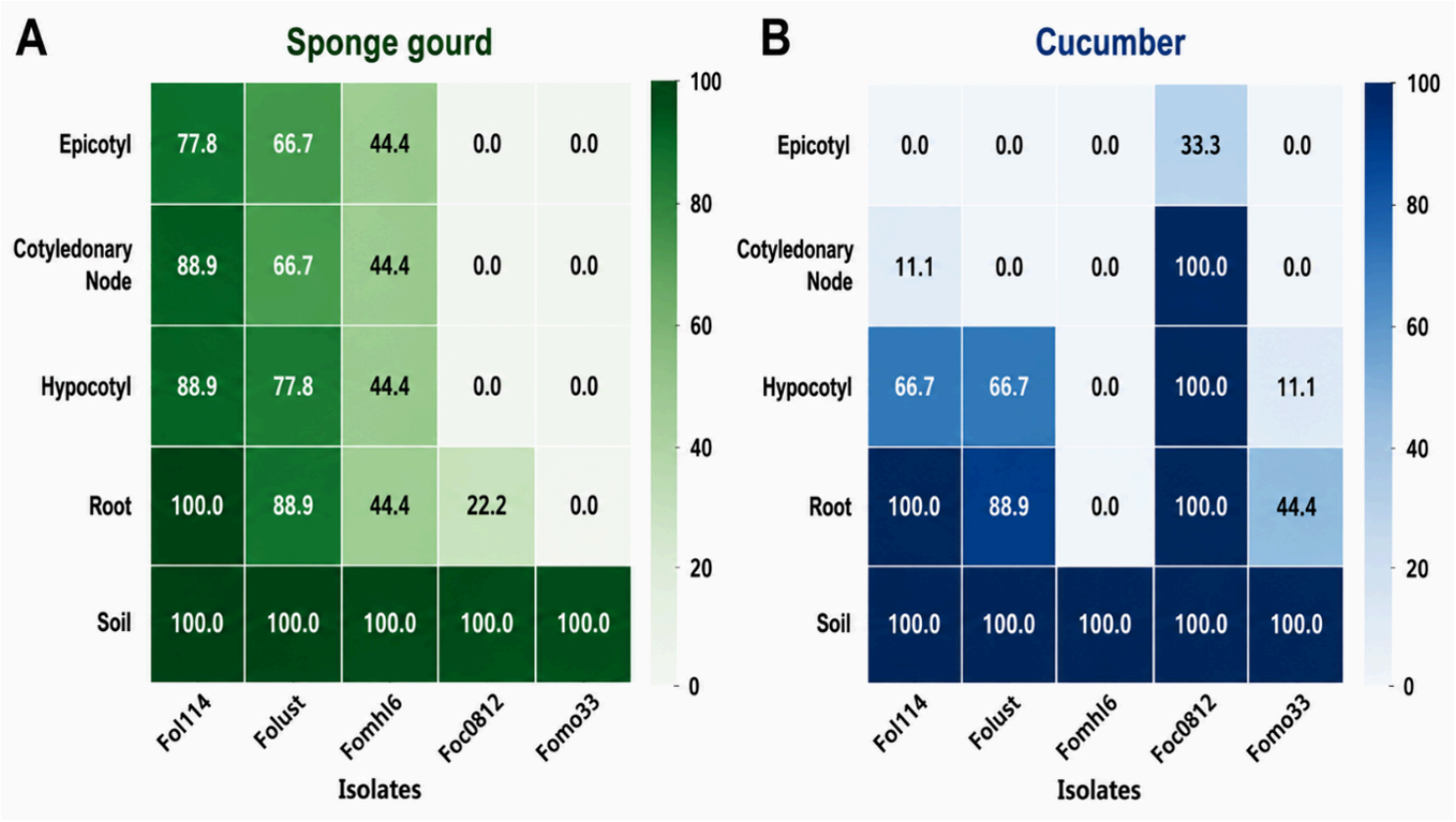


Figure 2

Tissue colonization frequencies of five representative *Fusarium oxysporum* isolates in sponge gourd (cv. OP) and cucumber (cv. VT) following soil infestation. Tissue colonization frequencies (%) were determined by pathogen re-isolation from five sampling positions, including the epicotyl, cotyledonary node, hypocotyl, root, and surrounding infested soil, 14 days after inoculation. A. Sponge gourd (cv. OP). B. Cucumber (cv. VT). Numbers within each cell indicate the percentage of pathogen re-isolation from each sampling position, and color intensity represents colonization frequency.

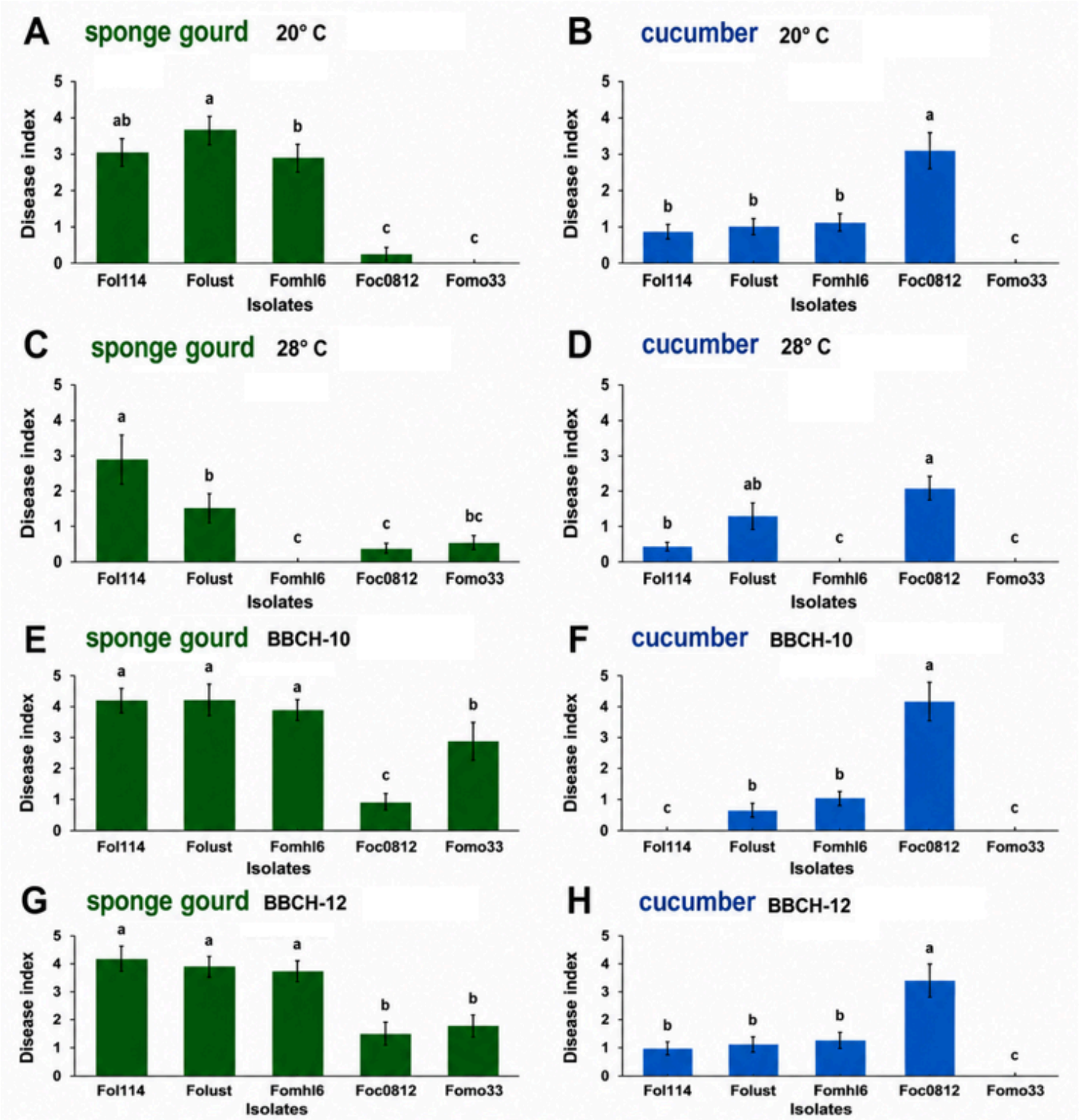


Figure 3

Effects of temperature and plant growth stage on disease severity caused by five representative *Fusarium oxysporum*isolates following root-dip inoculation.Disease severity was evaluated 14 days after inoculation using a 0–4 disease index (DI) scale. (A, B) Disease indices of sponge gourd (cv. OP) and cucumber (cv. VT) seedlings maintained at 20 °C. (C, D) Disease indices of sponge gourd and cucumber seedlings maintained at 28 °C. (E, F) Disease indices of seedlings inoculated at growth stage BBCH-10. (G, H) Disease indices of seedlings inoculated at growth stage BBCH-12. Error bars represent standard

deviations. Different letters indicate significant differences among isolates within each treatment according to one-way ANOVA followed by Tukey's HSD test ($P \leq 0.05$).

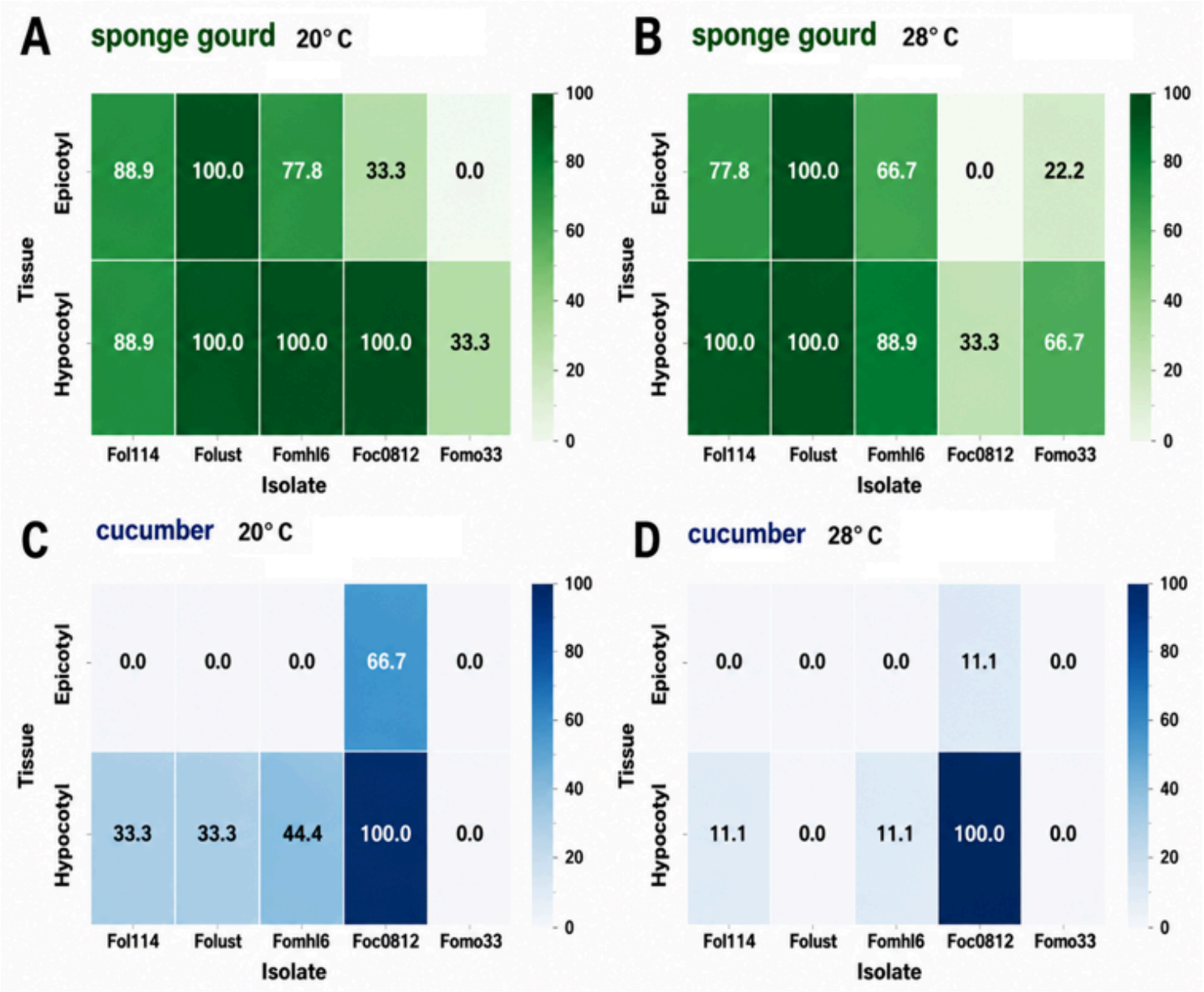


Figure 4

Tissue colonization frequencies of five representative *Fusarium oxysporum* isolates in sponge gourd (cv. OP) and cucumber (cv. VT) seedlings under two temperature regimes following root-dip inoculation. Tissue colonization frequencies (%) were determined by pathogen re-isolation from the hypocotyl and epicotyl tissues 14 days after inoculation. (A) Sponge gourd maintained at 20 °C. (B) Sponge gourd maintained at 28 °C. (C) Cucumber maintained at 20 °C. (D) Cucumber maintained at 28 °C. Numbers within each cell indicate the percentage of pathogen re-isolation from each tissue, and color intensity represents colonization frequency.

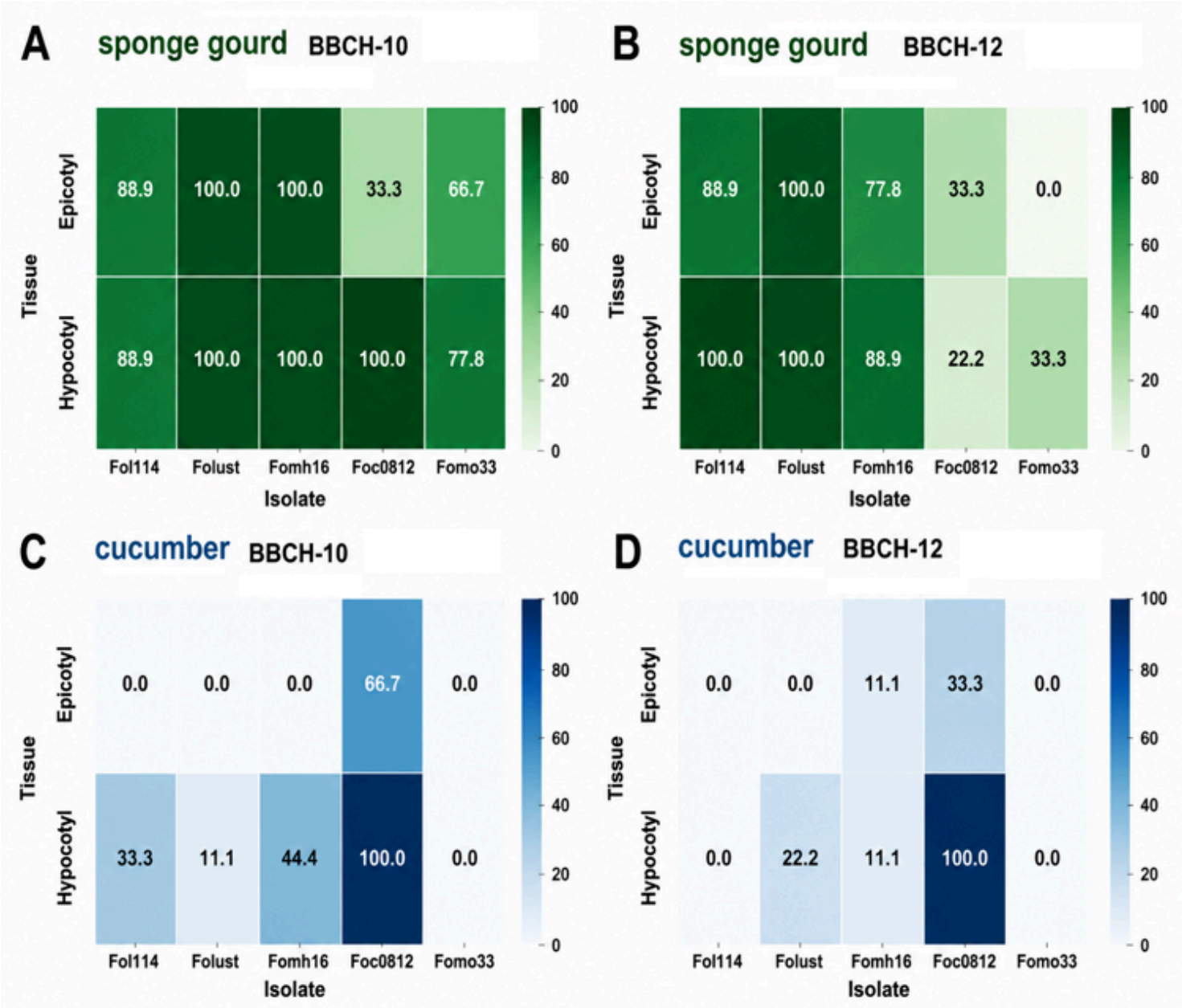


Figure 5

Tissue colonization frequencies of five representative *Fusarium oxysporum* isolates in sponge gourd (cv. OP) and cucumber (cv. VT) seedlings at two plant growth stages following root-dip inoculation. Tissue colonization frequencies (%) were determined by pathogen re-isolation from the hypocotyl and epicotyl tissues 14 days after inoculation. (A) Sponge gourd inoculated at BBCH-10. (B) Sponge gourd inoculated at BBCH-12. (C) Cucumber inoculated at BBCH-10. (D) Cucumber inoculated at BBCH-12. Numbers within each cell indicate the percentage of pathogen re-isolation from each tissue, and color intensity represents colonization frequency.

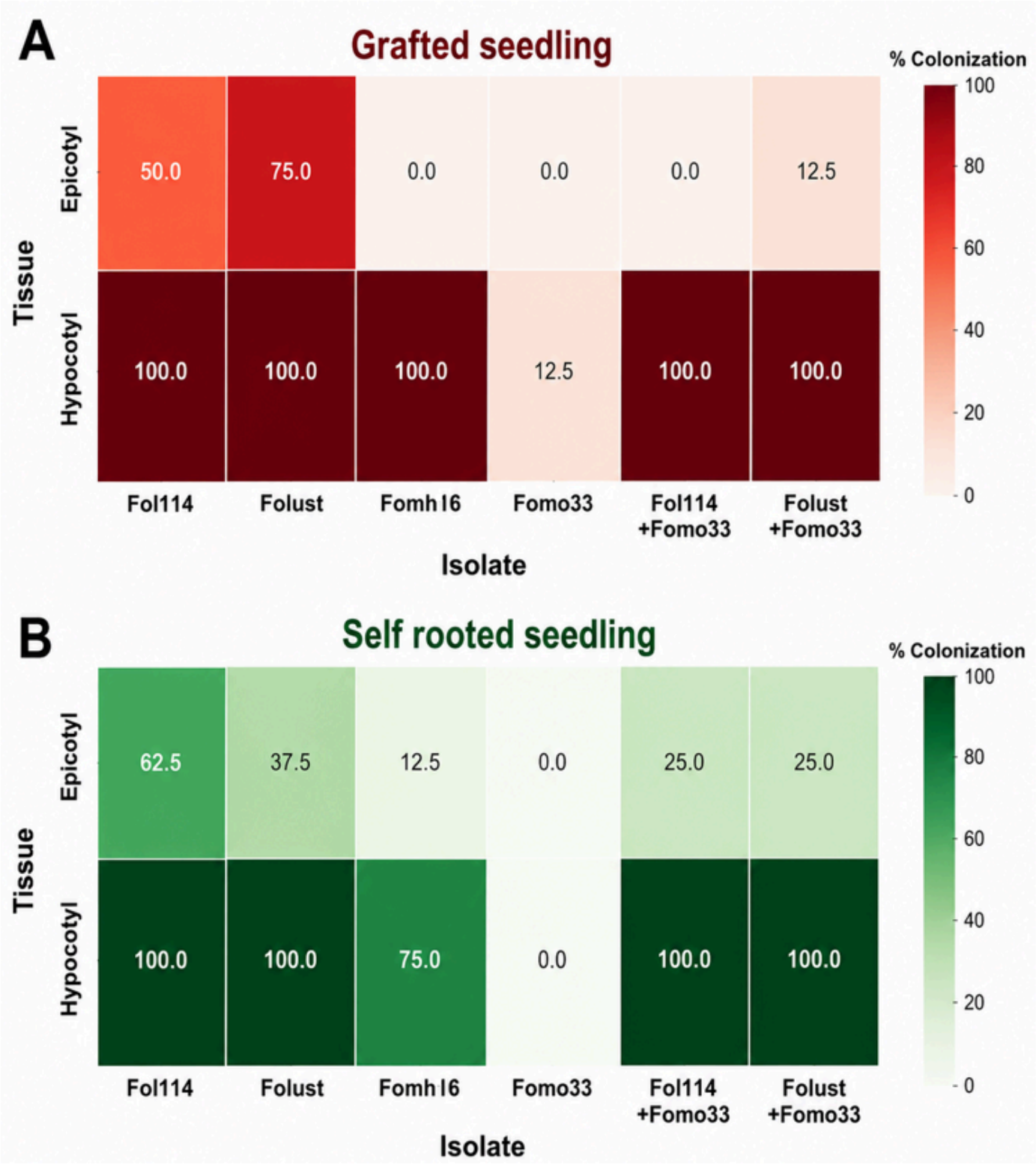


Figure 6

Effects of grafting on tissue colonization by representative *Fusarium oxysporum* isolates in grafted and self-rooted seedlings following soil infestation. Tissue colonization frequencies (%) were determined by pathogen re-isolation from hypocotyl and epicotyl tissues four weeks after inoculation. (A) Grafted bitter gourd scions on sponge gourd rootstocks. (B) Self-rooted sponge gourd seedlings. Numbers within each cell indicate the percentage of pathogen re-isolation, and color intensity represents colonization

frequency. For mixed-inoculation treatments, isolate-specific recovery frequencies determined by forma specialis-specific PCR are presented in Table 3.

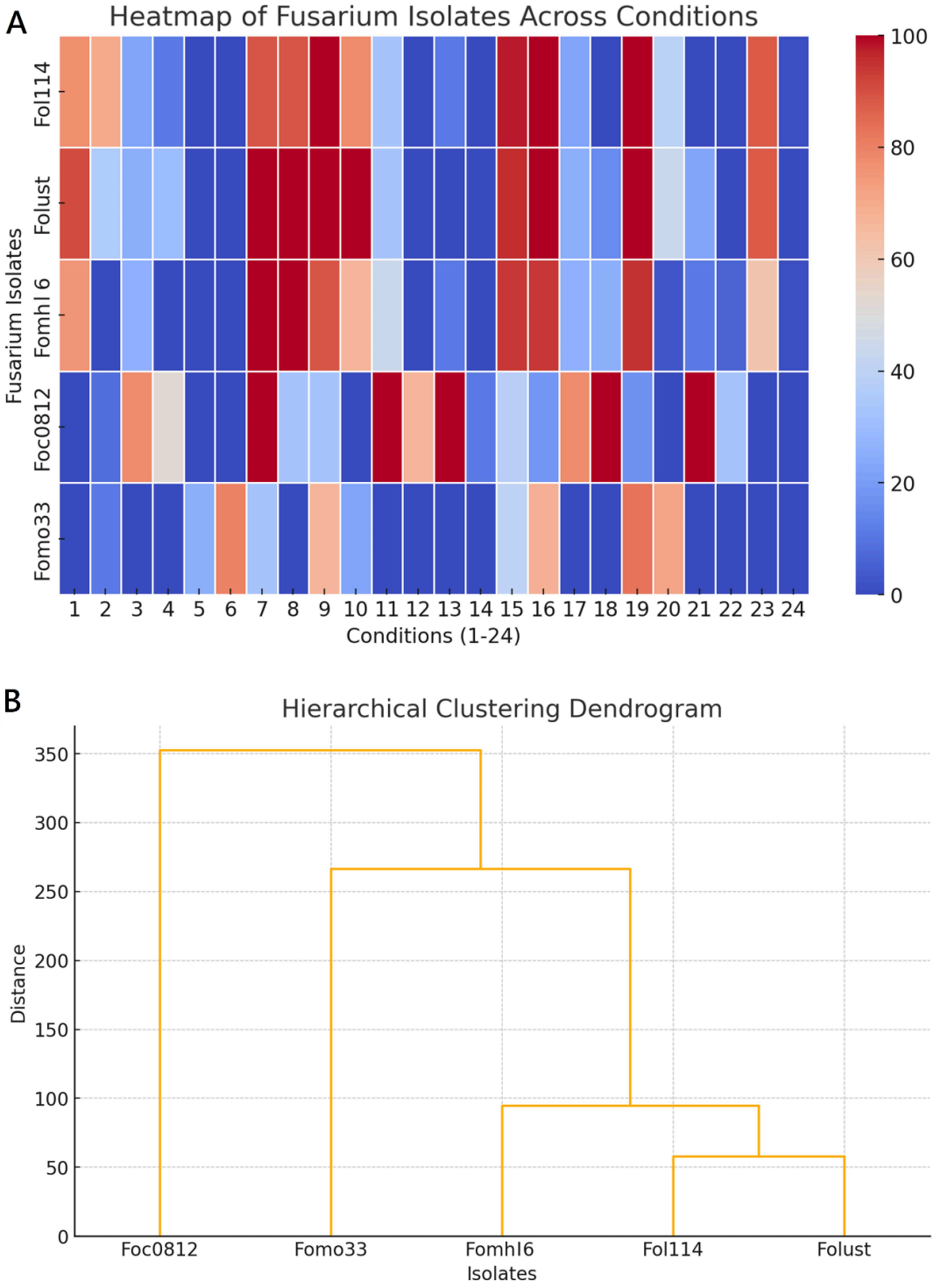


Figure 7

Integrated analysis of pathogenic responses of five representative *Fusarium oxysporum* isolates across 24 experimental conditions. (A) Heatmap illustrating normalized disease severity and tissue colonization

responses obtained from experiments involving different hosts, inoculation methods, temperature regimes, plant growth stages, and grafting systems. (B) Hierarchical clustering based on Euclidean distances using the integrated response matrix, illustrating similarities among isolates across all experimental conditions.

Note: Column numbers (1–24) in panel (A) correspond to the following distinct conditions:1–2 (Disease Index): Sponge gourd (20 °C), Sponge gourd (28 °C); 3–4 (Disease Index): Cucumber (20 °C), Cucumber (28 °C); 5–6 (Disease Index): Bitter gourd (20 °C), Bitter gourd (28 °C); 7–8 (Colonization at 20 °C): Sponge gourd hypocotyl, Sponge gourd epicotyl; 9–10 (Colonization at 28 °C): Sponge gourd hypocotyl, Sponge gourd epicotyl; 11–12 (Colonization at 20 °C): Cucumber hypocotyl, Cucumber epicotyl; 13–14 (Colonization at 28 °C): Cucumber hypocotyl, Cucumber epicotyl; 15–16 (Disease Index at BBCH): Sponge gourd (BBCH-10), Sponge gourd (BBCH-12); 17–18 (Disease Index at BBCH): Cucumber (BBCH-10), Cucumber (BBCH-12); 19–20 (Colonization at BBCH-12): Sponge gourd hypocotyl, Sponge gourd epicotyl; 21–22 (Colonization at BBCH-12): Cucumber hypocotyl, Cucumber epicotyl; 23–24 (Grafting Colonization): Grafted seedling hypocotyl, Grafted seedling epicotyl.

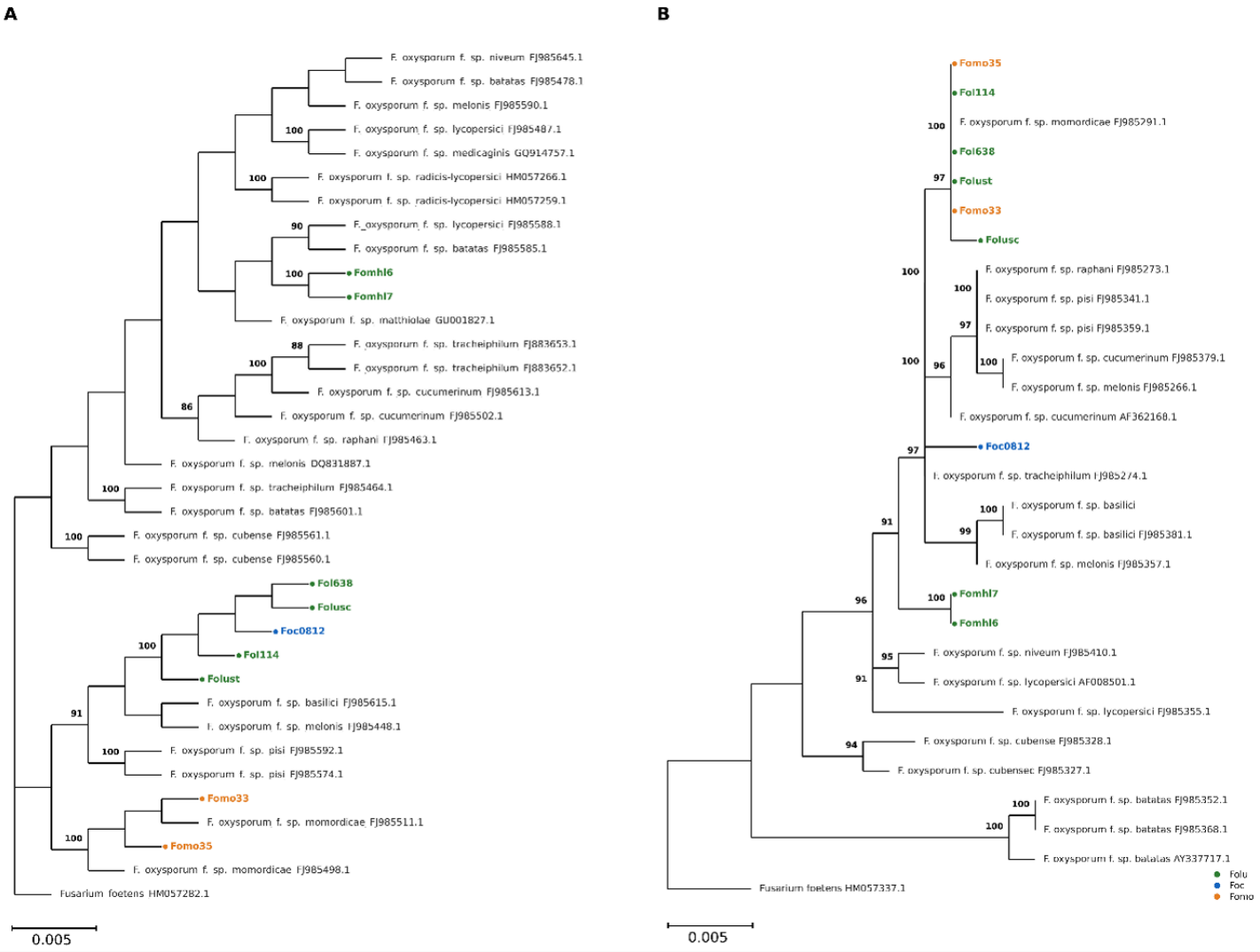


Figure 8

Phylogenetic analyses of representative *Fusarium oxysporum* isolates based on conventional molecular markers. Maximum-likelihood phylogenetic trees were constructed using (A) rDNA intergenic spacer (IGS) sequences and (B) *translation elongation factor 1-alpha* (*EF-1α*) sequences together with representative reference sequences retrieved from GenBank. Bootstrap values (>50%) based on 1,000 bootstrap replicates are shown at the corresponding nodes. *Fusarium foetens* was used as the outgroup.

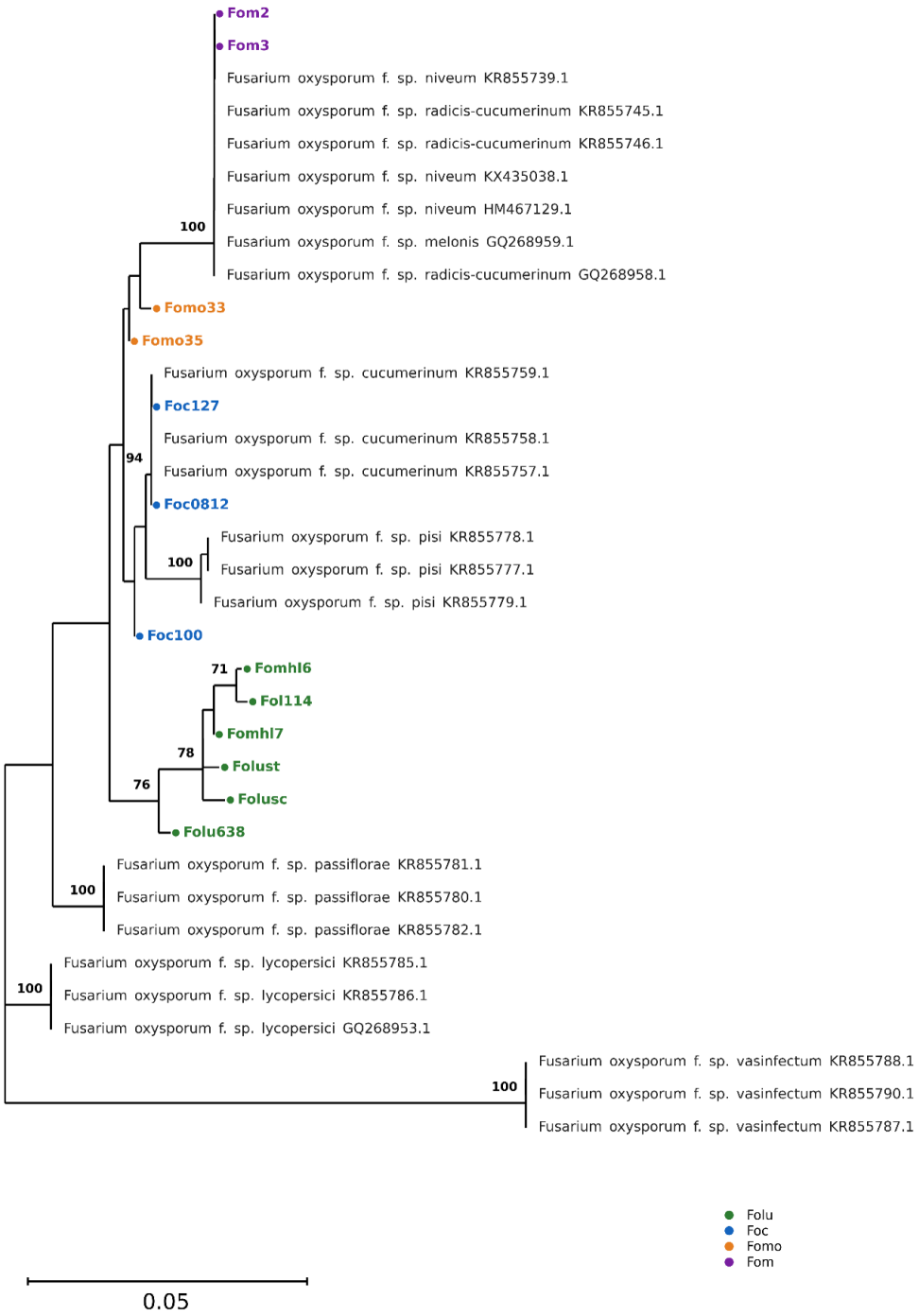


Figure 9

Phylogenetic analysis of representative *Fusarium oxysporum* isolates based on *SIX6*gene sequences. Maximum-likelihood phylogenetic analysis was performed using *SIX6* sequences from representative isolates included in this study together with representative reference sequences retrieved from GenBank. Bootstrap values (>50%) based on 1,000 bootstrap replicates are shown at the corresponding nodes. Colored labels indicate the representative isolates analyzed in this study.

Supplementary Files

This is a list of supplementary files associated with this preprint. Click to download.

- Tables.docx